

Article ID : 1001-4322(2005)01-0071-04

Simulation of Ne-like Ge 19.6 nm X-ray laser driven by picosecond laser pulse*

QIAO Xiu-mei¹, ZHANG Guo-ping², ZHANG Tan-xin²

(1. Graduate School of China Academy of Engineering Physics, P. O. Box 2101, Beijing 100088, China;

2. Institute of Applied Physics and Computational Mathematics, P. O. Box 8009, Beijing 100088, China)

Abstract : Transient collisional excitation (TCE) has proved to be an efficient method to significantly save driving energy. In this paper, Ne-like Ge 19.6 nm X-ray laser driven by picosecond Nd-glass laser pulse at 1.053 μm are simulated. The local gain greater than 60 cm^{-1} is predicted and calculations of the propagation of X-ray laser, including refraction effects, are done to understand which regions have the right combination of high gain and low density gradients for an optimum contribution to the X-ray laser output.

Key words : Transient collisional excitation; Gain; Refraction; X-ray Laser

CLC number : TN24 **Document code** : A

1 Introduction

X-ray laser has much shorter wavelength compared with other common optics laser, and as one kind of light source, it has better coherence, higher brightness and shorter pulse length (about several picoseconds) compared with other light sources in the same spectral range. It can be used in many fields, one of the important applications is to probe the electron density of warm and dense plasma^[1,2]. Using a Ni-like palladium X-ray laser at 14.7 nm produced interferograms of a dense (up to $2 \times 10^{20} \text{ cm}^{-3}$) and large (6 mm long) laser-produced plasma with a few picosecond temporal resolution^[1]. Whereas, the first X-ray laser was demonstrated on a huge laser facility NOVA in LLNL in 1984^[3] with two optics laser beams with $\sim 1 \text{ kJ}$ energy each, which makes X-ray laser unavailable to some laboratories or companies. To get more compact and cheaper X-ray laser, extensive experimental and theoretical works have been done since that time and significant advances have been made, especially in collisional excitation (CE) scheme. To dramatically save driving energy transient collisional excitation (TCE) was recently proposed^[4-7] and was first used to demonstrate lasing at 32.6 nm in Ne-like titanium at the Max Born Institute^[6], with less than 10 J of energy. In experiment, the hydrodynamic conditions of TCE scheme can be realized by using a low intensity long pre-pulse to produce a preplasma with rich populations of Ni-like or Ne-like ions in the ground state. After some delay time, a high intensity short pulse is used to make a jump of electron temperature. Because the gain duration is very short^[8], traveling wave pumping of the short pulse is necessary to synchronize the pump with X-ray laser along the target axis.

In this paper, we simulated the Ne-like Ge 19.6 nm X-ray laser by irradiating the 0.9 cm long Ge slab target with a 250 ps Nd-glass laser which was preceded by a 3% prepulse 4.5 ns earlier, and 40 ps later a 1 ps, 10 J high intensity short pulse heating the preplasma, a $\sim 100 \mu\text{m}$ wide and $\sim 1 \text{ cm}$ long focus line was produced. All the pulses were Gaussian at 1.053 μm in wavelength. The total energy of the double prepulses was 10 J, and the quasi-traveling wave pump for the short pulse was adopted.

2 Simulation Results

The one dimensional hydrodynamic code Jb 1 9 was used to calculate the hydrodynamic evolution of the plasma

* Received date : 2004-07-06 ; Revised date : 2004-10-27

Foundation item supported by National High-tech Research and Development Plan (863)

Biography: QIAO Xiu-mei (1976—), female, Ph. D., is engaged in the theoretical study of X-ray laser. E-mail: xiumeiq123@sina.com.

and provide the temperatures and densities to the recently developed N61 code, which performs the kinetics calculations to determine the gain. The 37 fine structure levels in the Ne-like Ge, 113 fine structure levels in F-like Ge with main quantum number n up to 3 and 12 fine structure levels in Na-like Ge with main quantum number n up to 4 were considered, for which the level energies and electron collisional excitation rates and radiation rates were provided by the Atomic Group of Institute of Applied Physics and Computational Mathematics (IAPCM). For higher excited states as well as other ions, the energies were calculated using the screened hydrogenic model, while the collisional and radiative rates were estimated using empirical formulas. To get the output intensity, the results were post-processed by the two dimensional paraxial ray-tracing code XPBA.

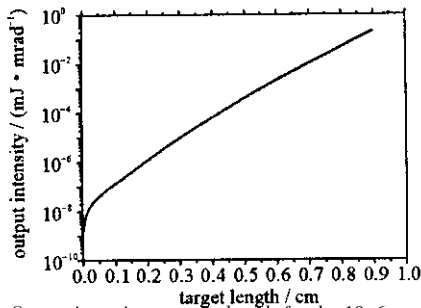


Fig. 1 Output intensity vs target length for the 19.6 nm line

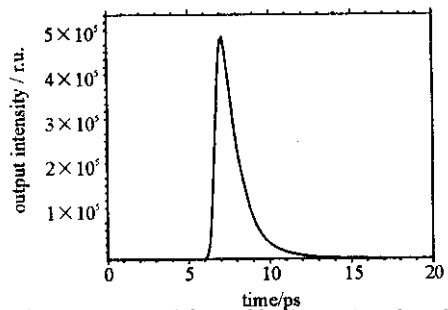


Fig. 2 Output intensity of the Ne-like Ge 19.6 nm laser line vs time

Figure 1 shows the analytical curves of the output intensity versus the target length based on the Linford formula^[10]. The small signal gain achieved is $\sim 19.5 \text{ cm}^{-1}$, and it decreases with the increase of the target length. The output energy is $9.5 \mu\text{J}$, the gain length product is ~ 17.5 , saturation is achieved.

Figure 2 shows the temporal distribution of the output intensity for the 19.6 nm X-ray laser. The short pumping pulse peaks at 6 ps on the horizontal axis. It indicates that the 19.6 nm laser output peaks 1.1 ps after the peak time of the short pulse and that the X-ray laser pulse length is ~ 1.5 ps. Figure 2 shows that the gain region, which contributes most to the output, is 1.1 ps after the peak time of the short pumping pulse. Figure 3 shows the plasma status at this time, including the variation of fraction of Ne-like ions and electron temperature and electron density versus distance from target surface. The dash-dot line in figure 6(b) shows the variation of gain at this time. It can be seen that the fraction of Ne-like ions in the gain region is larger than 0.6 and the electron temperature sharply increases to $\sim 1.8 \text{ keV}$ which results in the rapid rise of gain near the critical surface which is located at $10 \mu\text{m}$ on the horizontal axis. The largest gain achieved at this time is larger than 50 cm^{-1} , whereas this largest gain value contributes little to the output, because X-ray lines in this region will be bent out of the gain region as a result of severe refraction near the critical surface. To give more detailed illustration, figure 4 shows the tracing of the X-ray line which samples the largest gain-length product. Figure 4 also indicates that this line starts at $\sim 37.8 \mu\text{m}$ from target surface with a $\sim -6.9 \text{ mrad}$ incidence angle with the target normal direction, where the electron temperature is $\sim 1.4 \text{ keV}$, the electron density is $\sim 3.4 \times 10^{20} \text{ cm}^{-3}$ and the gain is 17.5 cm^{-1} and then it is bent inward to the target surface. At $\sim 15 \mu\text{m}$ from target surface, it samples the largest gain, $\sim 32 \text{ cm}^{-1}$, where the electron temperature is $\sim 1.76 \text{ keV}$, the electron density is $\sim 4.7 \times 10^{20} \text{ cm}^{-3}$ and the fraction of Ne-like ions is ~ 0.68 . After that it is bent outward away from the target surface. At $\sim 38.4 \mu\text{m}$ from the target surface, it travels out with an angle of $\sim 6.7 \text{ mrad}$ with the target normal direction and the gain-length product of this line is 21.5. The main gain region which contributes most to the output of this line is from $\sim 25 \mu\text{m}$ to $\sim 15 \mu\text{m}$ from the target surface where the gain is near 20 cm^{-1} and electron density is less than $5 \times 10^{20} \text{ cm}^{-3}$. It is also in this region that the X-ray line experiences severe refraction.

Figure 5(a) shows the dependence of the output intensity on the output position of the X-ray laser in the target normal direction and figure 5(b) shows the refraction angle dependence of the output intensity. One can see that the

output intensity peaks at $\sim 38 \mu\text{m}$ from target surface with the refraction angle of $\sim 6.8 \text{ mrad}$.

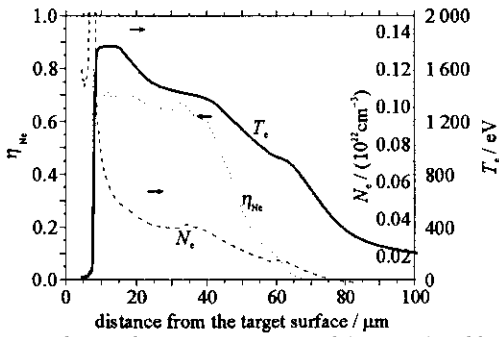


Fig. 3 Electron density , temperature and fraction of Ne-like ions 1.1 ps after the peak time of the short pulse

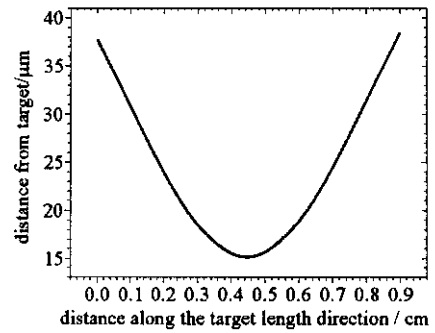


Fig. 4 Tracing of the line which samples the largest gain-length product

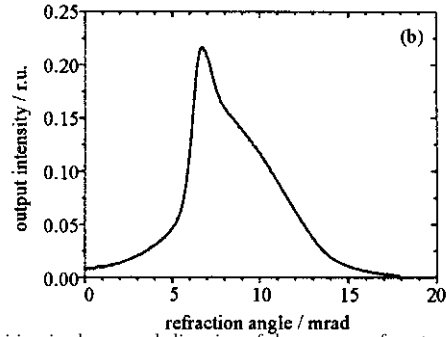
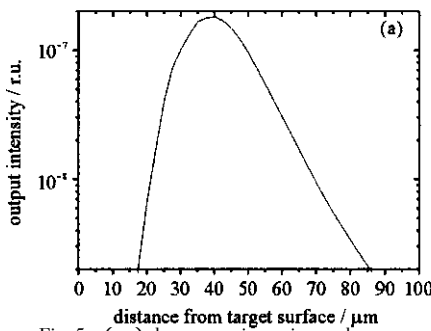


Fig. 5 (a) the output intensity vs the output position in the normal direction of the target surface ;
(b) the output intensity vs refraction angle for the Ne-like Ge 19.6 nm X-ray line

As enough Ne-like ions are produced by the two prepulses and the electron density and fraction of Ne-like ions do not vary very much in such a short time period , figure 6 shows the variation of electron temperature and gain as function of the distance from the target surface at the peak time of the short pulse (solid line) 0.4 ps (dash line) ; 1.1 ps (dash-dot line) ; 2 ps (dash-dot-dot line) and 3 ps (dot line) after the peak time of the short picosecond pulse. One can see that the electron temperature does not get the peak value until 0.4 ps after the peak time of the short pulse , resulting in the gain peaking at this time near the critical surface , whereas in the underdense region it is not very high. The temperature near the critical surface drops after 0.7 ps while in the underdense region it increases to get the largest value. Later on the electron temperature falls in the whole gain region. One important fact we must note is that though the gain peaks near the critical surface 0.4 ps after the peak time of the short pulse , the gain value in the main gain region as mentioned above is not the largest until 0.7 ps later as a result of the increase of the electron temperature , which accounts for why the output peaks 1.1 ps after the peak time of the short time.

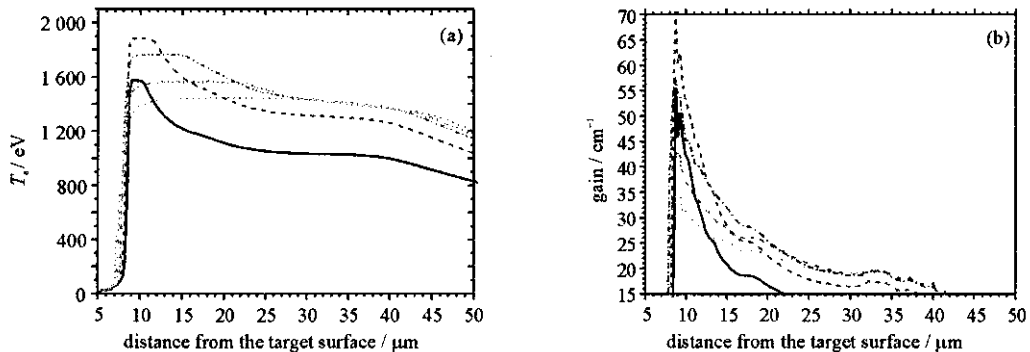


Fig. 6 Variation of electron temperature (a) and gain (b) as function of distance from the target surface at the peak time (solid line) ;
0.4 ps (dash-line) ; 1.1 ps (dash dot line) ; 2 ps (dash-dot-dot line) and 3 ps (dot line) after the peak time of the short pulse

We have tested our series code by simulating the experiments done by RAL in 2000 and in 1998^[9] , and have

compared our results with the experiment^[9], which is described in another in preparation. Comparison with the experiment shows that within the uncertainty in measuring the X-ray laser, our simulation agrees well with the experiment^[9], which suggests that our simulation in this paper is believable.

3 Summary

In this paper, we have simulated Ne-like Ge 19.6 nm X-ray laser line by irradiating ~0.9 cm-long slab target with two 250 ps prepulses that is followed 40 ps later by a ~1 ps drive pulse. The Jb19 code provides the densities and temperatures to the atomic kinetics code N61 which determines the gain. The results are post-processed by the ray-trace code XPBA. The temporal evolution of the plasma is studied. The output peaks 1.1 ps after the peak time of the short pulse and the pulse length of the 19.6 nm X-ray laser is only ~1.5 ps for which the main reason is the variation of electron temperature. Simulations predict gains ~19.5 cm⁻¹ and the output energy is ~9.52 μJ. Ray-tracing calculation shows that refraction effect is still one of the important factors affecting the TCE X-ray laser output.

The authors thank the Atomic Group of IAPCM for their atomic data and thank the coworkers in High Computation Center of IAPCM for the convenience they provided.

Reference :

- [1] Smith R F , Dunn J , Nilsen J , et al. Picosecond X-ray laser interferometry of dense plasma[J]. *Phys Rev Lett* , 2002 , **89** :065004.
- [2] Rocca J J , Hammarsten E C , Jankowska E , et al. Application of extremely compact capillary discharge soft X-ray lasers to dense plasma diagnostics [J]. *Physics of Plasmas* , 2003 , **10** :5.
- [3] Rosen M D , Hagelstein P L , Matthews D L , et al. Exploding-foil technique for achieving a soft X-ray laser[J]. *Phys Rev Lett* , 1985 **54** :106.
- [4] Afanasiev Y V , Shlyaptsev V N. Formation of a population inversion in Ne-like ions in steady-state and transient plasmas[J]. *Sov J Quant Electron* , 1989 , **19** :1606—1612.
- [5] Healy S B , Janulewicz K A , Plowes J A , et al. Transient high gains at 19.6 nm produced by picosecond pulse heating of a preformed germanium plasma[J]. *Opt Communications* , 1996 , **132** :442—448.
- [6] Nickles P V , Shlyaptsev V N , Kalachnikov M P , et al. Short pulse X-ray laser at 32.6nm based on transient gain in Ne-like titanium[J]. *Phys Rev Lett* , 1997 , **78** :2748—2751.
- [7] Dunn J , Osterheld A L , Shepherd R , et al. Demonstration of X-ray amplification in transient gain Nickel-like palladium scheme[J]. *Phys Rev Lett* , 1998 , **80** :2825—2828.
- [8] Klisnick A , Kuba J , Ros D , et al. Demonstration of 2 ps transient X-ray laser[J]. *Phys Rev A* , 2002 , **65** ,033810.
- [9] King R E , Pert G J , McCabe S P , et al. Saturated X-ray lasers at 19.0nm and 7.3nm pumped by a picosecond traveling-wave excitation[J]. *Phys Rev A* , 2000 , **64** :053810.
- [10] Linford G J , Peressini E R , Soody W R , et al. Very long lasers[J]. *Appl Opt* , 1974 , **13** :379.

模拟 ps 激光驱动类氖锗 19.6 nm X 光激光

乔秀梅¹ , 张国平² , 张覃鑫²

(1. 中国工程物理研究院 研究生部 , 北京 100088 ; 2. 北京应用物理与计算数学研究所 , 北京 100088)

摘要 : 瞬态电子碰撞激发产生 X 光激光的机制可以极大减少 X 光激光的泵浦能量。模拟了脉宽为 1 ps , 波长 1.053 μm 的钨玻璃激光驱动类氖锗 X 光激光。模拟表明 , 在临界面附近可以产生高达 60 cm⁻¹ 的增益 , 还计算了 X 光激光在等离子体中的传播 , 计算表明 X 光激光在等离子体中的折射效应仍然是影响 X 光激光输出强度及分布的重要因素。

关键词 : 瞬态电子碰撞激发 ; 增益 ; 折射 ; X 光激光